University of Baghdad
College of Engineering
JOURNAL OF ENGINEERING

Journal of Engineering
journal homepage: www.jcoeng.edu.iq

Volume 32 Number 1 January 2026

Optimal Weaving Lengths for Improved Traffic Flow Efficiency on Urban Arterial Roads: Case Study, Sulaymaniyah City, Kurdistan Region, Iraq

Bakhtiar Tahir Tofiq Al barznji , **Hirsh M. Majid** *

Department of Civil Engineering, College of Engineering, University of Sulaimani, Sulaymaniyah, Kurdistan Region, Iraq

ABSTRACT

Efficient design of weaving sections is critical for maintaining smooth traffic flow on urban arterial roads. This study investigates optimal weaving lengths (WL) for improving traffic flow efficiency using two weaving sections located on Malik Mahmud Ring Road in Sulaymaniyah City, Kurdistan Region, Iraq, as a case study. Traffic and geometric data were collected through drone footage and processed using data from Sky Viewer to extract detailed vehicle trajectories. A calibrated and validated microsimulation model was developed in PTV VISSIM 2024 to replicate real-world traffic conditions. A full factorial experimental design tested the effects of WL, mainline traffic volume, and weaving volume on section performance. The results demonstrated that WL significantly influences both capacity and level of service (LOS). Shorter sections constrained lane-changing maneuvers, while longer sections enhanced throughput and improved LOS; however, excessive length beyond 750 m for Section A and 350 m for Section B yielded diminishing returns. Regression analysis confirmed that the interaction between WL and volume ratio (VR) positively and significantly affected capacity, while higher VRs independently reduced efficiency. Section A achieved a stronger model fit (R^2 = 0.771) compared to Section B (R^2 = 0.650), reflecting site-specific geometric and traffic characteristics. The findings suggest that WLs of approximately 750 m for Section A and 350 m for Section B represent optimal design values for balancing roadway capacity and operational efficiency. This research provides a methodological framework for capacity estimation in weaving sections and offers practical insights for transportation planners and engineers in developing urban contexts.

Keywords: Urban arterial roads, WL, Traffic flow efficiency, VISSIM, Capacity estimation.

1. INTRODUCTION

Weaving sections on urban arterial roads play a critical role in traffic operations by allowing vehicles from different lanes to merge and diverge. When properly designed, these sections

*Corresponding author
Peer review under the responsibility of University of Baghdad.
https://doi.org/10.31026/j.eng.2026.01.03

Article received: 16/07/2025
Article revised: 11/10/2025
Article accepted: 20/10/2025
Article published: 01/01/2026

improve traffic efficiency and safety by reducing travel times, minimizing fuel consumption, and lowering congestion, thereby decreasing the overall ttransport cost in cities **(Anas and Lindsey, 2011)**. In addition, weaving sections facilitate multimodal transport systems—supporting buses, motorcycles, and other modes, which are essentiall for sustainable urban mobility**(Alessandretti et al., 2023)**. Conversely, poorly designed weaving sections can exacerbate traffic jams and increase the likelihood of accidents **(Olmos et al., 2018)**. Studies further suggest that appropriate weaving section design enhances safety outcomes: for example, bus travel, much of which occurs in these sections, has lower injury rates than private vehicle travel **(Morency et al., 2018)**. Thus, weaving sections are not only operational necessity but also central to the efficiency and safety of urban transport systems.

On urban arterial roads, insufficient WL has been associated with congestion and elevated accident risks. Short WLs force sudden lane changes, providing limited time for drivers to adjust speed or alignment, thereby increasing the risk of collisions **(Iamtrakul et al., 2023; Lampo et al., 2021)**. As urban areas expand, arterial highways intersect with core roadways, producing bottlenecks that intensify congestion **(Lampo et al., 2021)**. At the same time, sustainable urban planning requires balancing traffic efficiency, safety, and environmental considerations, making the optimisation of WLs a pressing challenge **(Hess et al., 2023; Loo and Tsoi, 2022)**.

Recent advances in intelligent transport systems and sensing technologies offer promising solutions. Integrating Ad Hoc vehicle networks with smart city infrastructure has been proposed to optimize traffic flow and improve road safety **(Paes et al., 2023; Yu et al., 2023)**. Optimising WLs can reduce vehicle delays, improve average operating speeds, and enhance the resilience of traffic systems in metropolitan areas **(Zhao et al., 2022)**. Beyond efficiency, it contributes to environmental sustainability by reducing emissions and supporting cleaner urban environments **(Dhar, 2023; Guzek et al., 2022)**.

This study employed the microscopic traffic simulation software VISSIM to create a simulation model of a case study on urban arterial weaving sections. Vissim is microscopic, behavior-based, stochastic, multi-functional traffic microsimulation software designed for simulating complex transportation projects. The model was built and adjusted with field data. The calibrated model served as a testbed for assessing various configurations and properties of arterial weaving sections via an experimental approach.

The objective of this study is to evaluate and optimize weaving section performance on urban arterial roads in Sulaymaniyah City by identifying optimal WLs through calibrated VISSIM microsimulation, supported by field data.

Weaving sections are widely recognized as critical points in urban road networks due to their high susceptibility to traffic conflicts and congestion, primarily caused by intensive lane-changing and merging maneuvers. Research has shown that unmanaged weaving operations significantly increase the risk of crashes and delays, highlighting the importance of advanced control strategies such as intelligent traffic management systems and real-time monitoring to enhance efficiency and safety **(Franco et al., 2018; Taillanter and Barthelemy, 2023)**. At the microscopic level, several studies have focused on driver behavior and lane-changing dynamics, which play a central role in weaving performance. **(Keane and Gao, 2021)**, for instance, identified the relaxation phenomenon in lane-changing, where drivers adjust their car-following behavior post-lane-change to stabilize headway variations. Similarly, **(Feng et al., 2023)** enhanced cellular automata models by accounting for different driving styles, demonstrating that aggressive behavior can increase roadway capacity, thereby underscoring the importance of behavioral heterogeneity in WL optimisation.

Beyond individual vehicle interactions, macroscopic and network-level models have also been employed to examine weaving section performance. **(Kerner, 2015)** further analyzed instabilities at highway bottlenecks, revealing nucleation phenomena that trigger tran sitions between synchronized and free flow traffic states, which must be considered when determining optimal WLs. **(Laurent-Brouty et al., 2020)** proposed a Hamilton–Jacobi-based model that integrates buffers, emphasizing the effects of spillback and junction dynamics. Complementing these approaches, **(Leclercq et al., 2021)** developed dynamic avoidance maps to optimize routing, offering practical strategies to manage weaving-related bottlenecks across urban networks.

Despite such advancements, weaving research continues to face several methodological and data-related challenges. A persistent limitation is the scarcity of detailed microscopic data; concerns over data validity and representativeness often lead to biased conclusions about t raffic dynamics **(Giest and Samuels, 2020)**, while shortcoming in data collection methodologies have been shown to generate erroneous inferences in traffic research **(Petracca and Frair, 2017)**. Moreover, urban environments pose unique challenges for modeling, as existing frameworks often fail to capture turbulence-like complexities, limiting the transferability of results across different spatial contexts **(Di Bernardino et al., 2015)**. Collectively, the literature suggests that while minimum WLs are essential to reduce con gestion and ensure safety, defining optimal WLs requires consideration of driver heterogeneity, traffic flow instabilities, and broader network-level interactions.

Current gaps—such as limited data resolution, methodological inconsistencies, and inadequate representation of diverse urban contexts—underline the need for improved data acquisition, advanced modeling frameworks, and empirical calibration. Addressing these limitations will enhance the realism and applicability of weaving section simulations, ultimately enabling the development of evidence-based WL optimisation strategies that can support safer, more efficient, and sustainable urban traffic systems.

2. METHODOLOGY

The methodology is delineated in four primary steps. The initial phase involves data collection, using two weaving sections located on Malik Mahmud Ring Road in Sulaymaniyah City, Kurdistan Region, Iraq, as the case study area. The sections comprise an urban arterial road characterized by traffic weaving conditions. The data collected encompassed geometric layout and traffic characteristics. Data collection employs videotaping methods. In the second phase of this study, the collected data were used to develop, calibrate, and validate a microsimulation model for the case study section .

In the third step, an experimental design was implemented to evaluate alternative traffic and geometric characteristics of urban arterial weaving sections. The analysis considered several factors: main road volume, entry ramp volume, ramp-to-ramp volume, and the length of weaving sections .

The final step involves analyzing the results and developing an empirical model for capacity estimation. The outputs of the developed model were compared to those of the conventional HCM 2022 procedure to evaluate its potential. **Fig. 1** illustrates the details of the applied methodology in this study.

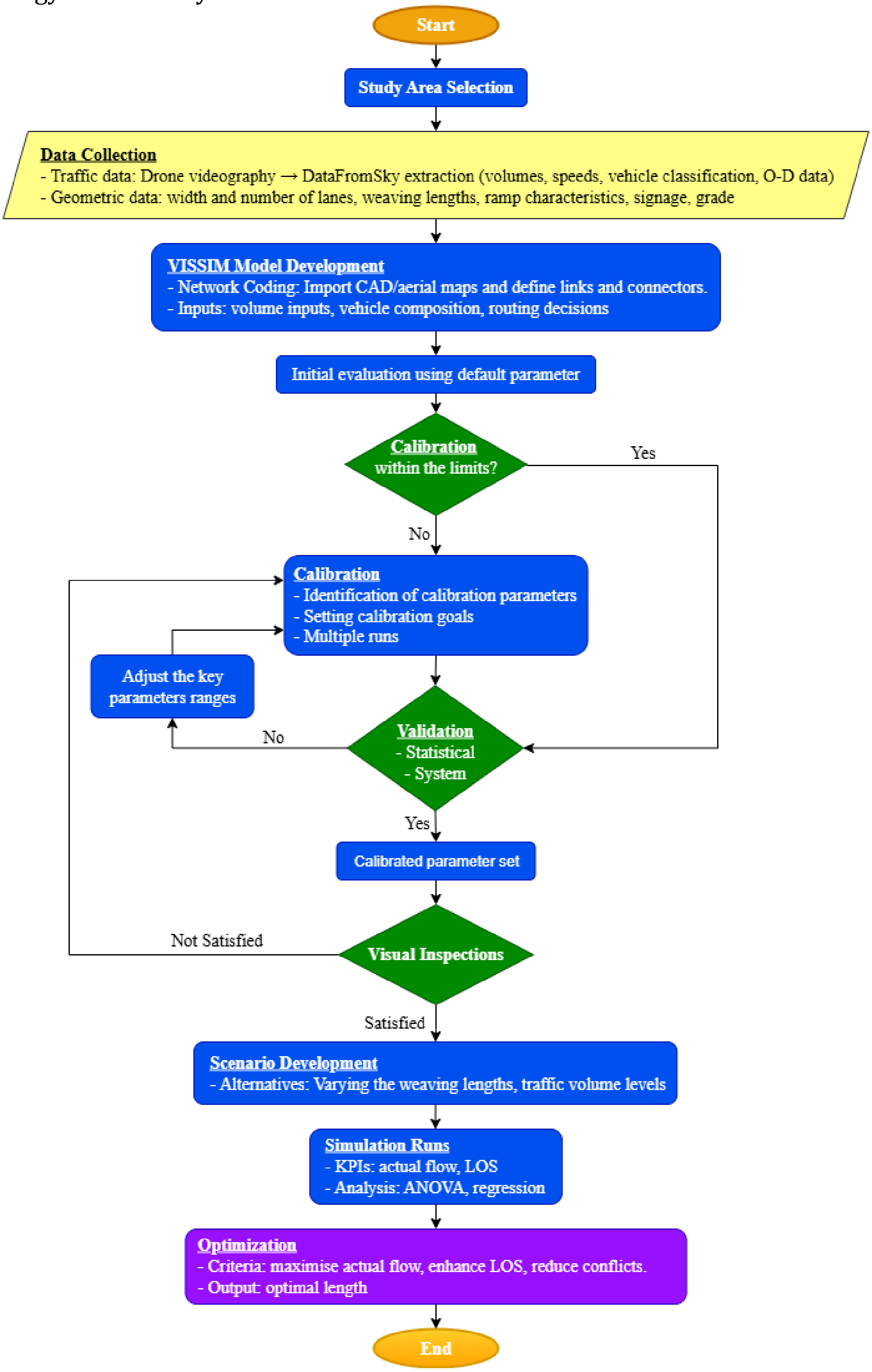

Figure 1. Flowchart of the research methodology.

2.1 Study Area and Data Collection

To achieve the objective of this research, two weaving sections on a major urban arterial roadway, Malik Mahmud Ring Road, Sulaymaniyah City, Kurdistan Region, Iraq, were selected. The site was chosen based on its observed weaving maneuvers and its geometric suitability for a VISSIM-based microsimulation analysis. The corridor is classified as a main arterial road with a 60 km/h speed limit according to the AASHTO classification system **(Hancock and Wright, 2013)**. The corridor in this section includes a main road and two service roadways. This section has six-lane separated arterial and two lanes for the service roadway (3.5 m lane width). The connections between the service and main roadways exist at specific locations. Two weaving sections of 185 m and 110 m in length were considered for weaving sections (A) and (B), respectively. The selected weaving sections are categorized as having a two-sided configuration, as described in HCM 2022 **(Manual, 2022)**. **Fig. 2** illustrates the layout of the selected weaving sections of the arterial road.

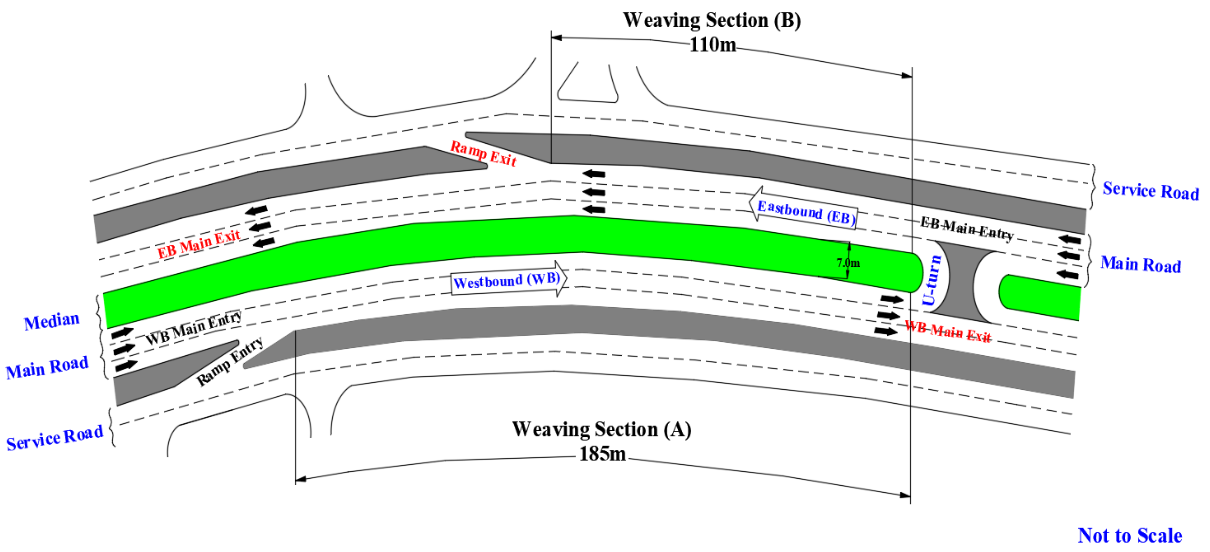

Figure 2. Layout of the investigated site (Malik Mahmud Ring Road, Sulaymaniyah, Kurdistan Region, Iraq).

Data collection was carried out through technological means. Drone footage was utilized to capture real-time traffic movement, enabling the accurate extraction of traffic volume, traffic composition, and speed data. This video data was processed using DataFromSky Viewer as shown in **Fig. 3**, which provided detailed trajectory-level information such as vehicle speeds, lane-changing behavior, and travel times. The traffic data was gathered during typical weather conditions and while the roadway surface was dry.

Additionally, geometric data of the roadway, including width and number of lanes, WLs, ramp characteristics, signage, and grade, was obtained from aerial maps and the site. These data points form the foundation for building and calibrating the simulation model in PTV VISSIM.

Figure 3. Processing of video data collected by using DataFromSky Viewer

2.2 Simulation Modelling Approach

To evaluate the impact of WL on traffic flow efficiency for urban artery roads, a microscopic traffic simulation modeling approach was adopted from the PTV VISSIM 2024 software. VISSIM is a highly flexible and widespread traffic pattern modeling program that is being used for the study of traffic management plans at a detailed, vehicle level **(Al Barznji and Majid, 2025; Boxill and Yu, 2000)**. Due to its aspect of being able to simulate individual driver characteristics and car interactions, VISSIM is particularly well-suited for studying complex traffic phenomena such as weaving. Initially, a base model was implemented to simulate the selected weaving section according to geometric and traffic data that were extracted from the site.

2.2.1 VISSIM Model Development

PTV VISSIM 2024, a behavior-based, microscopic simulation program that mimics individual vehicle movements based on car-following and lane-changing logic, was employed for the creation of a detailed traffic simulation model, which served as the analytical basis of this study. In weaving sections, where driver investment profoundly influences performance and safety, that level of detail becomes imperative for effectively characterizing dynamic traffic behaviors. VISSIM is best suited for the simulation of urban networks due to its ability to model a host of traffic components, i.e., private vehicles, public transport, pedestrians, bicycles, and a number of traffic control devices. Field demand was integrated in the model, consistent with developed protocols, such as the simulation protocols of the WSDOT and the Traffic Analysis Toolbox of the FHWA **(Dowling et al., 2004; Schilperoort et al., 2014)**. Network coding was the first step of the procedure, which involved importing CAD diagrams and high-definition aerial pictures of study areas for generating precise layouts of links, connectors, and weaving areas. Road sections were characterized through links, whereas lane changing and merging/diverging behaviors were simulated through connectors. Special emphasis was given to precisely describing the weaving sections, including geometry, accompanied by lane arrangements. The model included field demand based on established guidelines, which specified the desired speed for each section and the types and numbers of vehicles at each entry point. Vehicles could travel along specific paths in the network based on routing decisions that were predetermined from observed origin-destination (O-D) movements. Realistic flow through the intricate artery system was replicated through static routing assignments. The following categories of calibration parameters are considered:

1. Basic calibration parameters, including simulation resolution.
2. Car Following parameters.
3. Lane change parameters.
4. Lateral behavior.
5. Desired speed distributions.

2.2.2 Base Model Calibration and Validation

In order that simulated outputs reflect real-world traffic accurately, a necessary step that goes into the traffic simulation modelling process is calibration. Calibration was employed in this study to calibrate VISSIM model parameters so that its output is aligned with field data readings, thus complementing the model's predictiveness and integrity. Mimicking traffic flows and volume properly, representing decent car speeds and travel intervals, and reproducing the characteristic lane-changing and weaving actions seen in the study area were the main goals of the calibration process. Car-following and lane-changing behaviors consisted of the two major parameter sets that were subject to calibration. Three parameters (average standoff distance, additive component of safety distance, and multiplicative component of safety distance) were calibrated across the site chosen to capture regional car-following action better, according to the adoption of the Wiedemann 74 model, which is suitable for use on urban arterials, as shown in **Table 1**. Simulation properly captures the realism of real-world traffic flow characteristics of weaving sections through parameter variation.

Table 1. Calibration parameters with selected values.

Type	Parameter	Unit	Default Value	Selected Values
Simulation parameters - General	Simulation resolution	Time Steps/sim. sec.	10	10
	Random seed	-	42	42
	Random seed increment	-	1	1
Driving Behaviour Car Following	Average standstill distance	m	2	2.2
	Additive part of safety distance	m	2	2
	Multiplicative part of safety distance	m	3	3
Driving Behaviour Lane-Change	Lane Change Distance for downstream connectors	m	185 (weaving section A)	
			110 (weaving section B)	
Driving Behaviour Lateral	Observe adjacent lanes	-	option selected	
	Diamond queuing	-	option selected	
	Consider next turn	-	option selected	
	Overtake left	-	option selected	
	Overtake right	-	option selected	
Desired Speed	Desired speed distribution	kph	(55 – 65)	

A systematic calibration and validation procedure was used to establish the confidence and reliability of the VISSIM model, taking into consideration the inherent variability brought on by varying random seed values in microsimulation runs, as shown in **Tables 2 and 3**.
In accordance with WSDOT guidelines **(Schilperoort et al., 2014).** An initial sample of 11 simulation runs was carried out to make sure the average results were statistically representative and unaffected by outliers. With confidence intervals based on permitted departures from actual observations in terms of traffic volume and travel times, a 95% confidence level was chosen. Carefully chosen simulation parameters included a 3600-minute runtime after a 15-minute warm-up to achieve steady-state conditions. The necessary number of simulation runs was calculated using a formula from FHWA's Traffic Analysis Toolbox **(Dowling et al., 2004)**, as shown in Eq. (1), and the first 11 runs were found to be adequate.

$$N = \left(2 * \mathrm{t}_{0.025,N-1} \frac{s}{R}\right)^2 \tag{1}$$

R = Confidence Interval for the true mean
$t_{0.025,N-1}$ = Student's t-statistic for two-sided error of 2.5 percent (totals 5 percent) with N-1 degrees of freedom (this is related to a 95% Confidence Level)
s = Standard Deviation about the mean for selected MOE
N = Number of required simulations runs

Traffic volumes and travel times were used as effectiveness metrics during the iterative process of calibrating the model to match field data. To ensure the reliability of this process, the GEH statistic was calculated for all traffic volumes at every entry and exit location within the calibration area of the model. The accuracy of traffic volumes was then evaluated by computing the GEH values according to Eq. (2), and all results were found to fall within the permissible GEH threshold of 3.

$$GEH = \sqrt{\frac{2(m-c)^2}{(m+c)}} \tag{2}$$

m = output traffic volumes from the simulation model (vph)
c = traffic volumes based on field data (vph)

Table 2 compares the field volumes to the calibrated VISSIM outputs from the 11 simulation runs.
Confirming the model's calibration, model travel times also matched field data within allowable tolerances based on interrupted flow facility criteria according to Eq. (3) as follows:

$$\Delta = \frac{1}{\frac{1}{t} - \frac{0.1*5280\,S}{3600\,L}} - t \tag{3}$$

Δ = Allowable Travel Time Variation (+/- seconds)
t = Travel Time (seconds)
L = Length (feet)
S = Posted Speed (mph)=37.28

Table 2. Traffic volume calibration/validation results.

Process	Weaving section	Description	"Field" Volume (vph)	Average simulation Volume (vph)	GEH	Calibration Test
Calibration	A	WB Ramp Enry	304	304	0.0	Pass
		WB Main Entry	1960	1961	0.0	Pass
		WB Main Exit	1904	1889	0.3	Pass
		U-turn Exit	360	376	0.8	Pass
Validation	B	U-turn Entry	360	376	0.8	Pass
		EB Main Entry	3048	3034	0.3	Pass
		EB Ramp Exit	360	363	0.2	Pass
		EB Main Exit	3048	3044	0.1	Pass

Table 3 provides a comparison of the VISSIM collected travel times to the field collected travel times. The VISSIM data differed from the field data by less than the allowable variation defined in the calibration/validation goals. Thus, a calibrated and validated model offers a reliable basis for scenario analysis and design suggestions.

Table 3. Travel Time calibration/validation results

Process	Weaving Section	Average "Field" Travel Times (sec)	Average simulation Travel Time (sec)	Difference	Allowable Travel Time Variation (+/- seconds)	Calibration Test
Calibration	A	13.135	12.671	-0.46	+/- 1.64	Pass
Validation	B	9.292	8.781	-0.51	+/- 1.38	Pass

2.3 Assessment of Speed Estimation Methods for Urban Arterial Weaving Sections

Fig. 4 shows the average speeds for two weaving sections (A and B) that were observe from field data, calculating according to the HCM2022 methodology, and output from the VISSIM simulation. The average speed observed from the field data for Section A was 50.70 kph, which is lower than both the HCM-estimated speed (56.82 kph) and the VISSIM-simulated speed (52.56 kph). The field average speed for Section B was 42.62 kph, but the HCM predicted a much higher value (54.65 kph), and VISSIM estimated a value that was closer but still higher (45.10 kph).

In general, the results show that the HCM methodology always overestimates average speeds compared to field data, while VISSIM simulations demonstrate values that are more in line with the real-world data. This indicates that microscopic simulation can more accurately represent real-world traffic dynamics compared to the generalized HCM model, especially in weaving sections where driver behavior and lane-changing interactions significantly affect traffic flow. The differences also show how important it is to calibrate and validate models when using simulation tools to test and improve the performance of weaving sections on urban arterial roads.

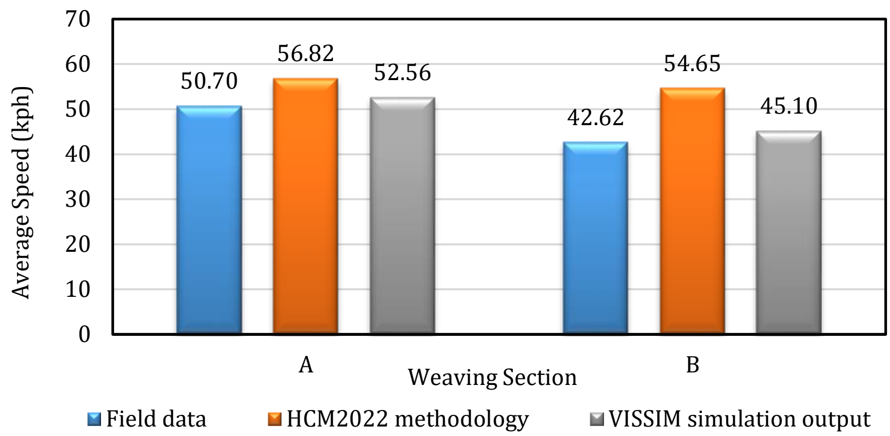

Figure 4. Comparison of Average Speeds from Field Observations, HCM Estimates, and VISSIM Simulations for Weaving Sections A and B

2.4 Traffic Simulation

A full factorial experiment design was adopted to test the effect of 3 factors on the weaving section actual flow, namely: weaving section length, main road traffic volume, and ramp-to-ramp volume (weaving volume). The levels of these factors are as follows:

1. Weaving section A
   - Weaving section length: 8 levels (150 m, 250 m, 350 m, 450 m, 550 m, 650 m, 750 m, and 850 m).
   - Main road volume: 4 levels (1000 vph, 2000 vph, 3000 vph, and 4000 vph).
   - Ramp-to-ramp volume (weaving volume): 4 levels (200 vph, 300 vph, 400 vph, vph, and 500 vph).
2. Weaving section B
   - Weaving section length: 4 levels (150 m, 250 m, 350 m, and 450 m).
   - Main road volume: 4 levels (1000 vph, 2000 vph, 3000 vph, and 4000 vph).
   - Ramp-to-ramp volume (weaving volume): 4 levels (200 vph, 300 vph, 400 vph, 500 vph, and 600 vph).

The level of the weaving section length remains continuous until the flow and LOS stability are achieved.

Table 4 shows the simulation scenario matrix for each weaving section length, which includes 16 combinations of traffic volume. In total, 128 and 64 experimental scenarios were tested and evaluated for weaving sections (A) and (B), respectively. 11 replicate simulation runs were conducted for each experimental scenario using different random seed numbers to minimize any random error.

Table 4. Different combinations of traffic volumes per waving section length

Scenario No.	V_M (Main volume) (vph)	V_W (weaving volume) = V_{RR} (Ramp-to-Ramp volume) (vph)	Total volume (V_M + V_{RR}) (vph)
1	1000	200	1200
2		300	1300
3		400	1400
4		500	1500
5	2000	200	2200
6		300	2300

7		400	2400
8		500	2500
9	3000	200	3200
10		300	3300
11		400	3400
12		500	3500
13	4000	200	4200
14		300	4300
15		400	4400
16		500	4500

3. RESULTS AND DISCUSSION

3.1 Results of Simulation Scenarios

Fig. 5 summarizes the results of the simulation-based investigation. The figure illustrates the correlation between total volume (demand) and actual flow across various weaving volumes (200 vph, 300 vph, 400 vph, and 500 vph) for weaving section lengths of 150 m and 850 m for weaving section A and 150 m and 450 m for weaving section B as a case study. Demand is characterised as the total traffic volume seeking to utilize the weaving section, specifically the sum of the main road traffic volume and the entrance ramp traffic volume to the main road. Conversely, actual flow denotes the real flow that may effectively traverse the weaving section. Simulation tools do not yield capacity directly. The sole method to assess the capacity of a certain system component via simulation is to subject it to overload and ascertain the maximum flow under such conditions. Consequently, the capacity derived from simulation is regarded as the maximum flow associated with the weaving volume for a specified length of weaving section. **Fig. 5** illustrates that flow increases with the increase in sectional total volume until a certain limit or threshold is reached. Beyond this limit, no additional vehicles could be accommodated, resulting in a stable flow. This threshold may be considered the section capacity or maximum flow under overloaded conditions.

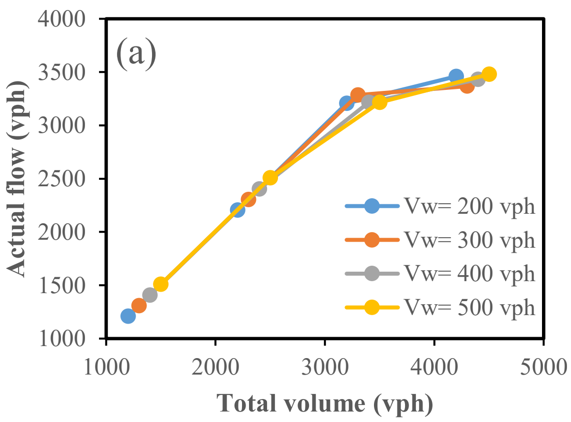

(a) WL = 150 for weaving section A

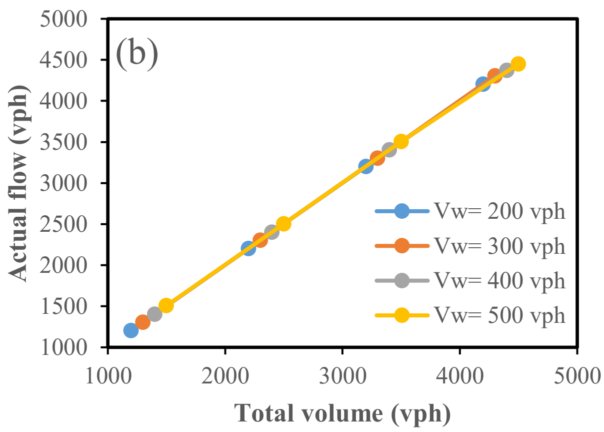

(b) WL = 850 for weaving section A

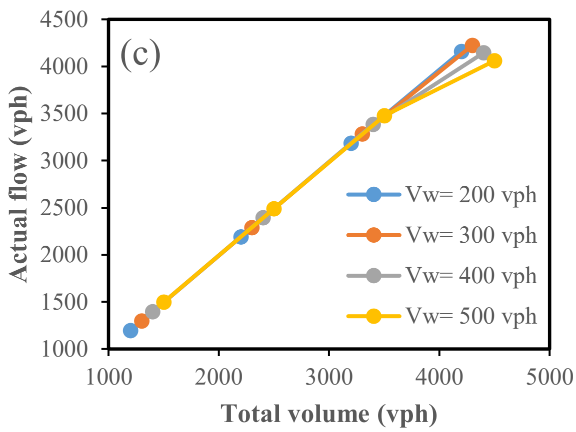

(c) WL = 150 for weaving section B

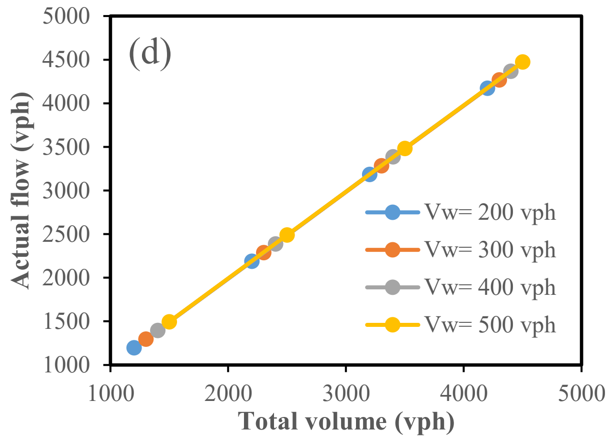

(d) WL = 450 for weaving section B

Figure 5. Simulation results (Total volume versus actual flow)

The illustration further indicates that an increase in the weaving volume corresponds to a decrease in the threshold. This signifies less capacity under high weaving volume. The WL seems to enhance the sectional capacity. This can be attributed to the fact that the increased length enables smooth, lane-changing manoeuvres before reaching the exit ramp. **Table 5** presents the maximum flow for each VR throughout all WLs, derived from capacity estimations obtained from simulation runs under diverse weaving scenarios. The table indicates that an increase in VR diminishes section capacity, with this decrease differing over various WL, particularly at high VR values.

Table 5. Capacity estimations from simulation scenarios.

	Weaving Section A							
VR	**Maximum flow or Capacity (vph)**							
	WL = 150 m	WL = 250 m	WL = 350 m	WL = 450 m	WL = 550 m	WL = 650 m	WL = 750 m	WL = 850 m
200	3460	3916	4200	4204	4200	4204	4204	4204
300	3368	3560	4128	4284	4304	4304	4308	4308
400	3432	3348	3732	4204	4380	4404	4400	4372
500	3480	3432	3736	4004	4264	4308	4436	4452
	Weaving Section B							
VR	**Maximum flow or Capacity (vph)**							
	WL = 150 m		WL = 250 m		WL = 350 m		WL = 450 m	
200	4160		4172		4172		4172	
300	4224		4272		4272		4268	
400	4144		4364		4368		4368	
500	4060		4452		4472		4472	

Fig. 6 illustrates the relationship between WL (m) and level of service (LOS value) for different weaving volumes (200, 300, 400, and 500 vph):

- For the weaving section A, the figure shows that LOS improves (lower LOS values) as WL increases, though the rate and extent of improvement vary with traffic volume. At lower weaving volumes (200 vph), LOS decreases sharply with increasing length, reaching stable values around LOS 1–2 once the length exceeds 350 m, indicating efficient traffic operations. For 300 vph, a similar pattern is observed, with LOS improving significantly between 250 m and 450 m before stabilising at LOS values of about 1.5. At 400 vph, the decline in LOS is more gradual, with notable improvements occurring only after 350 m, and the LOS levels off around 2 beyond 650 m. For the highest volume (500 vph), LOS remains relatively high at shorter WLs, showing only modest improvement as length increases, with values fluctuating between 3.5 and 4.5 beyond 450 m. These results highlight that longer weaving sections generally enhance LOS performance, but the benefits diminish at higher traffic volumes, where operational efficiency is constrained even with extended WLs.

- For weaving section B, the results indicate that increasing WL significantly improves LOS across all traffic volumes. At shorter WLs (150 m), the LOS values are relatively high, particularly at higher traffic volumes (e.g., Vw = 500 vph reaches close to LOS = 2.5). As WL increases to 250 m and beyond, LOS values sharply decline toward approximately 1.0, reflecting improved traffic conditions and smoother flow. Beyond 350 m of WL, the LOS stabilizes near 1.0 for all volume levels, suggesting that longer weaving sections effectively mitigate congestion and lane-changing conflicts regardless of traffic intensity. This trend highlights the critical importance of providing adequate WLs to sustain high levels of operational efficiency, especially under high traffic demand.

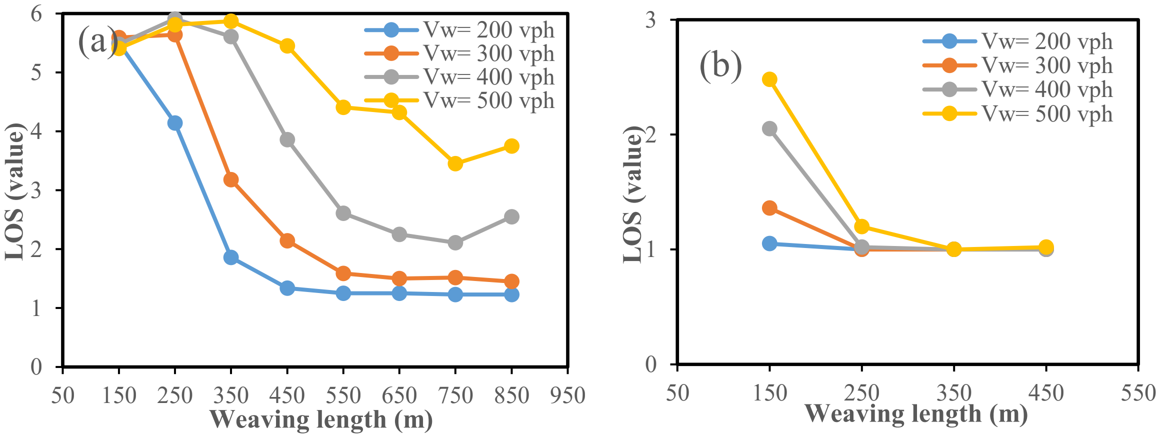

(a) (b)

Figure 6. Simulation results (WL versus LOS): (a)weaving section A, (b)weaving section B

3.2 Models for Capacity Estimation

Using Microsoft Excel, a regression analysis was performed on the simulation's data to determine a connection between capacity and the various influencing factors **(Berk and Carey, 2000)**. WL and VR were designated as the independent factors, and capacity as the dependent variable. Regression analysis, t-test(*P*-value), R^2, and F(*P-value*) results for capacity estimation models for sections A and B are shown in **Table 6.**

Having applied the previous criteria, the linear regression model between capacity, WL, and VR is given as follows:

$$C_w = \beta_0 + \beta_1 (WL * VR) + \beta_2 VR \quad (4)$$

where:

C_w = weaving section capacity (vph)

β_0, β_1 , β_2 = regression coefficients

WL = weaving length (m)

VR = volume ratio = weaving volume/ total volume

Table 6. Results of the linear regression models for capacity estimation

Weaving Section	Independent Variable	Coefficients		t(*P*-value)	R^2	F (*P*-value)
		symbol	value			
A	Intercept	β_0	4129.492	36.307(0.000)	0.771	48.699 (0.000)
	WL * VR	β_1	16.666	9.841(0.000)		
	VR	β_2	-9351.938	-5.820(0.000)		
B	Intercept	β_0	4071.471	91.385(0.000)	0.650	26.045 (0.000)
	WL * VR	β_1	8.527	5.103(0.000)		

The regression results presented in **Table 6** provide insights into the relationship between weaving section performance and the independent variables tested.

- For Weaving Section A, the regression model demonstrates a strong explanatory power with an R^2 value of 0.771, indicating that 77.1% of the variation in the dependent variable is explained by the model. The F-statistic of 48.699 (p = 0.000) confirms that the model as a whole is statistically significant. The coefficients reveal important effects:
  - The intercept (β_0 = 4129.492, t = 36.307, p = 0.000) is highly significant, representing the base capacity when other variables are at zero.
  - The interaction term WL × VR (β_1 = 16.666, t = 9.841, p = 0.000) has a positive and significant influence, suggesting that the combined effect of WL and VR contributes positively to capacity.
  - Conversely, the VR variable alone (β_2 = -9351.938, t = -5.820, p = 0.000) exerts a strong negative impact, implying that higher VRs reduce the overall capacity of the section. This aligns with weaving theory, where higher weaving volumes typically increase turbulence and reduce performance efficiency.
- For Weaving Section B, the model also shows statistical significance, though with a comparatively lower explanatory power (R^2 = 0.650). This indicates that about 65.0% of the variance is explained by the model, which is still acceptable but weaker than Section A. The F-statistic (26.045, p = 0.000) confirms overall model validity. Key findings include:
  - The intercept (β_0 = 4071.471, t = 91.385, p = 0.000) is again highly significant, providing the baseline estimate.
  - The interaction term WL × VR (β_1 = 8.527, t = 5.103, p = 0.000) remains positively significant, though the coefficient is smaller than in Section A, indicating a less pronounced combined effect of WL and VR on capacity.

Comparing the two sections, it is evident that Section A exhibits a stronger model fit and a more substantial influence of the interaction effect compared to Section B. The negative coefficient of VR in Section A but not in Section B highlights differences in geometric design factors between the two sections.

4. CONCLUSIONS

This study analyzed weaving section performance on urban arterial roads in Sulaymaniyah City, Iraq, to determine optimal WLs that improve traffic flow. Using drone-based data collection, DataFromSky trajectory extraction, and PTV VISSIM 2024 simulations, two weaving sections were modeled under varied traffic and geometric conditions. Calibration and validation confirmed accurate representation of real-world behavior. Results showed that WL strongly influences capacity and LOS. Short sections restricted vehicle maneuvers and reduced flow, while longer ones improved efficiency up to an optimal point around 750 m for Section A and 350 m for Section B beyond which benefits diminished. Regression analysis indicated that WL and VR jointly enhanced capacity, although higher VR alone reduced performance in Section A. Model fit was stronger for Section A (R^2 = 0.771) than for Section B (R^2 = 0.650). The findings provide practical guidance for optimizing weaving designs in developing urban settings. However, the study's reliance on simulations and limited sites constrains its generalizability. Future research should include more corridors, diverse traffic modes, and the impacts of connected and autonomous vehicles. Overall, the research emphasizes the value of WL optimization for improving mobility, safety, and efficiency in rapidly expanding cities like Sulaymaniyah.

NOMENCLATURE

Symbol	Description	Symbol	Description
Δ	Allowable Travel Time Variation (± seconds)	PTV VISSIM	Microscopic traffic simulation software used to model individual vehicle behavior
C_w	Weaving section capacity (vph)	R	Confidence interval for the true mean
CAD	Computer-Aided Design	R^2	Coefficient of determination
F	F-statistic from regression analysis to test model validity as a whole	s	Standard deviation about the mean of selected measure of effectiveness (MOE)
FHWA	Federal Highway Administration	S	Posted speed limit (mph)
GEH	Geoffrey E. Havers statistic (for traffic volume validation)	t	Observed or simulated travel time (seconds)
HCM	Highway Capacity Manual	t Stat	Statistical measure to evaluate the significance of each regression coefficient
L	Length of the travel segment (feet)	$t_{0.025, N-1}$	Student's t-statistic for 95% confidence level in simulation run estimation
LOS	Level of Service	vph	Vehicles per hour
MOE	Measure of Effectiveness	VR	Volume Ratio
N	Number of required simulations runs	WSDOT	Washington State Department of Transportation
O-D	Origin-Destination	WL	Weaving Length (m)

Acknowledgements

The authors acknowledge the help and support from the College of Engineering, University of Sulaimani, to complete this research work.

Credit Authorship Contribution Statement

Bakhtiar Tahir Tofiq Al barznji: Writing – review & editing, Writing – original draft, Validation, Software, Methodology. Hirsh M. Majid: Supervision, Review and academic guidance.

Declaration of Competing Interest

The authors declare that they have no known competing financial interests or personal relationships that could have appeared to influence the work reported in this paper.

REFERENCES

Al Barznji, B.T.T., and Majid, H.M., 2025. Comprehensive review and future directions in the analysis and optimization of weaving areas on urban arterial roads. *Current Problems in Research*, 1(1), pp. 1-25. https://doi.org/10.70028/cpir.v1i1.18.

Alessandretti ,L., Natera Orozco, L.G., Saberi, M., Szell, M., and Battiston, F., 2023. Multimodal urban mobility and multilayer transport networks. *Environment and Planning B: Urban Analytics and City Science*, 50(8), pp. 2038-2070. https://doi.org/10.1177/23998083221108190.

Anas, A., and Lindsey, R., 2011. Reducing urban road transportation externalities: Road pricing in theory and in practice. *Review of Environmental Economics and Policy*. https://doi.org/10.1093/reep/req019.

Berk, K.N., and Carey, P., 2000. *Data Analysis with Microsoft Excel*. Duxbury Press Pacific Grove, CA.

Boxill, S.A., and Yu, L., 2000. An evaluation of traffic simulation models for supporting its. *Houston, TX: Development Centre for Transportation Training and Research, Texas Southern University*, P. 25.

Dhar, P. 2023. Scientists are engineering Asphalt that is safer for humans and the environment. *ACS Publications*.

Di Bernardino, A., Monti, P., Leuzzi, G., and Querzoli, G., 2015. Water-channel study of flow and turbulence past a two-dimensional array of obstacles. *Boundary-Layer Meteorology*, 155(1), pp. 73-85.

Dowling, R., Skabardonis, A., and Alexiadis, V., 2004. Traffic analysis toolbox, volume III: Guidelines for applying traffic microsimulation modeling software. United States. Federal Highway Administration. Office of Operations.

Feng, T., Liu, K., and Liang, C., 2023. An improved cellular automata traffic flow model considering driving styles. *Sustainability*, 15(2), P. 952. https://doi.org/10.3390/su15020952.

Franco, S., Lindsay, A., Vallati, M., and McCluskey, T.L., Year. An innovative heuristic for planning-based urban traffic control. In Computational Science–ICCS 2018: *18th International Conference*, Wuxi, China, June 11–13, 2018, Proceedings, Part I 18, pp. 181-193. *Springer*.

Giest, S., and Samuels, A., 2020. 'For good measure': data gaps in a big data world. *Policy Sciences*, 53(3), pp. 559-569.

Guzek, M., Jurecki, R.S., and Wach, W. 2022. Vehicle and traffic safety. *MDPI*. 4573.

Hancock, M.W. and Wright, B., 2013. A policy on geometric design of highways and streets. *American Association of State Highway and Transportation Officials: Washington, DC, USA*, *3*, p. 20.

Hess, P., Piper, M., and Sorensen, A., 2023. Can we retrofit suburban arterials? analyzing the walkability and retrofit potential of four toronto region corridors. *Journal of the American Planning Association*, 89(1), pp. 16-30. https://doi.org/10.1080/01944363.2022.2033637.

Iamtrakul, P., Chayphong, S., and Mateo-Babiano, D., 2023. The transition of land use and road safety studies: a systematic literature review (2000–2021). *Sustainability*, 15(11), P. 8894. https://doi.org/10.3390/su15118894.

Keane, R., and Gao, H.O., 2021. A formulation of the relaxation phenomenon for lane changing dynamics in an arbitrary car following model. *Transportation Research Part C: Emerging Technologies*, 125, P. 103081. https://doi.org/10.1016/j.trc.2021.103081.

Kerner, B.S., 2015. Microscopic theory of traffic-flow instability governing traffic breakdown at highway bottlenecks: Growing wave of increase in speed in synchronized flow. *Physical Review E*, 92(6), P. 062827. https://doi.org/10.1103/PhysRevE.92.062827.

Lampo, A., Borge-Holthoefer, J., Gómez, S., and Solé-Ribalta, A., 2021. Emergence of spatial transitions in urban congestion dynamics. *Applied Network Science*, 6(1), P. 41.

Laurent-Brouty, N., Keimer, A., Goatin, P., and Bayen, A.M., 2020. A macroscopic traffic flow model with finite buffers on networks: Well-posedness by means of Hamilton-Jacobi equations. *Communications in Mathematical Sciences*, 18(6), pp. 1569-1604. https://dx.doi.org/10.4310/CMS.2020.v18.n6.a4.

Leclercq, L., Ladino, A., and Becarie, C., 2021. Enforcing optimal routing through dynamic avoidance maps. *Transportation Research Part B: Methodological*, 149, pp. 118-137. https://doi.org/10.1016/j.trb.2021.05.002.

Loo, B.P., and Tsoi, K.H., 2022. Road safety strategies necessary in the second Decade of Road Safety. *Journal of Global Health*, 12, P. 03081. https://doi.org/10.7189/jogh.12.03081.

Manual, H.C., 2022. Highway capacity manual. *Washington, DC*, 2(1), P. 1.

Morency, P., Strauss, J., Pépin, F., Tessier, F., and Grondines, J .2018 ,.Traveling by bus instead of car on urban major roads: safety benefits for vehicle occupants, pedestrians, and cyclists. *Journal of Urban Health*, 95, pp. 196-207.

Olmos, L.E., Çolak, S., Shafiei, S., Saberi, M., and González, M.C., 2018. Macroscopic dynamics and the collapse of urban traffic. *Proceedings of the National Academy of Sciences*, 115(50), pp. 12654-12661. https://doi.org/10.1073/pnas.1800474115.

Paes, V.d.C., Pessoa, C.H.M., Pagliusi, R.P., Barbosa, C.E., Argôlo, M., de Lima, Y.O., Salazar, H ,.Lyra, A., and de Souza, J.M., 2023. Analyzing the challenges for future smart and sustainable cities. *Sustainability*, 15(10), P. 7996. https://doi.org/10.3390/su15107996.

Petracca, L.S., and Frair, J.L., 2017. When methodological flaws limit inference: A response to Caruso et al. *Oryx*, 51(2), pp. 208-208. https://doi.org/10.1017/S0030605316000788.

Schilperoort, L., McClanahan, D., Shank, R., and Bjordahl, M., 2014. Protocol for VISSIM simulation. *Washington State Department of Transportation: Washington, DC, USA*.

Taillanter, E., and Barthelemy, M., 2023. Evolution of road infrastructure in large urban areas. *Physical Review E*, 107(3), P. 034304. https://doi.org/10.1103/PhysRevE.107.034304.

Yu, L., Zhang, Z., Li, J., Ma, J., and Wang, Y., 2023. A multi-objective roadside unit deployment model for an urban vehicular ad hoc network. *ISPRS International Journal of Geo-Information*, 12(7), P. 262. https://doi.org/10.3390/ijgi12070262.

Zhao, X., Hu, L., Wang, X., and Wu, J., 2022. Study on identification and prevention of traffic congestion zones considering resilience-vulnerability of urban transportation systems. *Sustainability*, 14(24), P. 16907. https://doi.org/10.3390/su142416907.

أطوال النسيج المثلي لتحسين كفاءة تدفق المرور على الطرق الشريانية الحضرية: دراسة حالة، مدينة السليمانية، إقليم كردستان، العراق

بختيار طاهر توفيق البرزنجي ، هيرش م. مجيد *

قسم الهندسة المدنية، كلية الهندسة، جامعة السليمانية، السليمانية، إقليم كردستان، العراق

الخلاصة

يُعد التصميم الفعّال لمناطق النسيج أمرًا حاسمًا للحفاظ على انسيابية تدفق المرور في الطرق الحضرية الرئيسة. تهدف هذه الدراسة إلى استقصاء الأطوال المثلى لمناطق النسيج بغرض تحسين كفاءة تدفق المرور، من خلال دراسة حالتين على الطريق ملك محمود الدائري في مدينة السليمانية، إقليم كردستان، العراق. جُمعت البيانات المرورية والهندسية باستخدام لقطات جوية عبر الطائرات المسيّرة، وتمت معالجتها ببرنامج DataFromSky Viewer لاستخراج مسارات المركبات التفصيلية. بعد ذلك، جرى تطوير نموذج محاكاة دقيقة مُعاير ومُتحقق من صحته باستخدام برنامج PTV VISSIM 2024 لمحاكاة ظروف المرور الواقعية. كما تم اعتماد تصميم تجريبي كامل العوامل لاختبار تأثير طول منطقة النسيج، وحجم المرور على الطريق الرئيسي، وحجم المرور المتشابك في أداء المقطع المدروس .أظهرت النتائج أن طول منطقة النسيج يؤثر بشكل ملحوظ في كل من السعة المرورية ومستوى الخدمة . إذ إن المقاطع الأقصر تُقيّد مناورات تغيير المسارات، بينما تسهم المقاطع الأطول في تعزيز معدل التدفق وتحسين مستوى الخدمة، إلا أن الزيادة المفرطة في الطول (تجاوز 750 م في المقطع A و350 م في المقطع B) لا تحقق فوائد إضافية ملموسة. كما أكّد تحليل الانحدار أن التفاعل بين طول منطقة النسيج ونسبة الحجم المروري يؤثر إيجابًا وبشكل ملحوظ في السعة المرورية، في حين أن النسب العالية للحجم المروري تؤدي إلى تقليل الكفاءة بشكل مستقل. وحقق المقطع A ملاءمة أفضل للنموذج ($R^2 = 0.771$) مقارنة بالمقطعB ($R^2 = 0.650$) ، وهو ما يعكس الخصائص الهندسية والمرورية الخاصة بكل موقع .تشير النتائج إلى أن الأطوال المثلى لمناطق النسيج تبلغ نحو 750م لمقطع A و 350م لمقطع B، وذلك لتحقيق التوازن بين السعة التشغيلية وكفاءة الأداء. وتوفر هذه الدراسة إطارًا منهجيًا لتقدير السعة في مناطق النسيج، كما تقدم رؤى عملية للمخططين والمهندسين في قطاع النقل ضمن البيئات الحضرية النامية.

الكلمات المفتاحية: الطرق الشريانية الحضرية، طول النسيج، كفاءة تدفق المرور، VISSIM، تقدير السعة.